EAI Endorsed Transactions
on Energy Web
Research Article EAI.EU

Static Voltage Stability Assessment of Ethiopian power System Using Normalized Active Power Margin Index

Ahadu Hilawie[1,*], Fekadu Shewarega[2]

[1]School of Electrical and Computer Engineering, Addis Ababa University, Addis Ababa, Ethiopia
[2]Institute of Electrical Power Systems, University of Duisburg-Essen, Duisburg, Germany

Abstract

Voltage stability assessments, made so far on the Ethiopian electric power system (EEP), are limited both in number and in methodology. Here, in this paper the static voltage stability of the Ethiopian power system is investigated using an index called normalized active power margin. The methodology starts from determining Thevenin equivalent of a system as viewed from the load buses. The Thevenin equivalent parameters help to determine the load bus maximum active power transfer limit and to draw the PV relation curves. The approach avoids the time-consuming method of PV curve based maximum active power transfer determination, which requires large number of power flow computations. The resulting maximum active power transfer and current operating active power load are used for the index calculation. The index is tested using IEEE 30 bus system and produced results matching with other previously established indices. The index is capable of ranking vulnerability of load buses to voltage instability. Then, scenarios of heavy load and light load EEP cases, with and without system reactive power compensation, are investigated. Results reveal weakest buses are supplied from 66kV transmission lines, load bus 232 being the weakest of all. On the other hand, the most stable buses are supplied from 132 kV transmission lines, bus 149 being the most stable bus. PV curves drawn, also, reveal the improvement that come with reactive power compensation and with operating in light load condition.

Keywords: Ethiopian power system, Voltage stability index, Thevenin equivalent, Maximum active power transfer.

Received on 25 March 2022, accepted on 31 October 2022, published on 15 December 2022

doi: 10.4108/ew.v9i40.141

1. Introduction

With the increasing global power demand, power systems have been experiencing a load dependent power system security problem, voltage instability. Voltage instability is characterized by uncontrolled voltage decline at load buses regardless of the amount of reactive power compensation switched to [1-3]. The voltage instability in any one bus of the power system may result in cascading events leading to total system collapse [4, 5].

To avoid the risk of system collapse, maintaining a safe distance from voltage instability is a necessary security insuring task of power system operators. The voltage security maintaining tasks require static voltage stability assessments to be made on the system. Static voltage stability assessments evaluate how far, current steady state operating point, is from point of voltage instability inception [6].

A number of methods and associated indices have been proposed by literature for assessing static system voltage stability [7, 8]. These indices consider either load buses [9-12] or transmission lines [13-15] for detecting voltage instability.

Indices measure the closeness of a system to voltage instability [16]. Mostly, this closeness is not interpretive to parameters known by system operators. To overcome this problem, this investigation is made by developing active power transaction based index. The index is understandable for a system operator who sees and manages problems in power related terms. Additionally, the index considers the main cause of voltage instability; active power loading.

*Corresponding author. Email: ahaduhiz@gmail.com,

The index, which is termed as active power margin index (PPMI), functions based on the idea of locating the maximum possible active power transfer. In most of PV based analysis techniques, the location of the maximum active power transfer performed by conducting repetitive power flow calculations through increasing the load until the power flow solution diverges [17-19]. However, this approach consumes considerable processing time and memory which is undesirable for fast operational computations, including online system monitoring. A continuation power flow method is also devised for locating the point of collapse [20-25]. However, this too requires considerable number of iterative computations to be performed.

In this work, the search of maximum active power transfer is made in two steps. The first step is the Thevenin equivalent determination, which uses only two power flow calculations. Next the maximum active power transfer is calculated in a deterministic way. The deterministic way avoids the requirement of large number of numerical iterations in this second step. The total low number of power flow computation makes the approach appealing for fast computational requirement [26].

The developed index is then tested on standard IEEE 30 bus test system. To validate the results other indices; impedance stability index (ISI) as in [9] and apparent power stability index (SPMI) according to [27] are used. The developed index produces a matching result with these benchmark indices.

Coming to the Ethiopian power system; it is a fast-growing power system. The system has two parts; The interconnected system (ICS) and the self-contained system (SCS), which are isolated grids.

The total generation capacity of the system currently reached 4500 MW and the peak load connected reached to be 2900 MW. The system operator, the Ethiopian Electric Power (EEP) is seeing a near future connectivity to a new grand hydropower generation. The new plant, Grand Ethiopian Renaissance Dam (GERD), has an installed capacity of 6500 MW which exceeds the total current generation by 1.45-fold.

The power generation seems in surplus for voltage instability to be a problem. However, three conditions make the surplus to get completely depleted. The first is the inland high connectivity demand. The existing connectivity is among the lowest in Africa. Only 46 % of the population has electricity [28], making the remaining 54 % to live in hope of future connectivity. The second condition is the government's ambitious plan of power sell and regional connectivity. The government planned to add power sell among the top export items. The third condition is the high-power loss within the system which consumes considerable MWs. The power loss within the system is estimated to be about 20 % [29].

The transmission system comprises transmission voltages of 45 kV, 66 kV, 132 kV, 230 kV, 400 kV and 500 kV. Among these, 66 kV transmission lines are old age lines and have high resistance per km as compared to other transmission voltages. This would, probably, contribute to the voltage instability problems [30].

Additionally, blackouts are recurring within the EEP. The blackout occurrence per year is high [31]. These conditions require voltage stability of the system to be rigorously assessed.

Despite the presence of these problems, stability assessment studies are not given due consideration by the system operator. Additionally, the papers, in the academia, that considered the issue are limited in number and methodology. It is tried to investigate voltage stability in EEP considering only the 230 kV transmission system in [32]. This, however, doesn't suffice to see the full picture of the problem within the EEP system.

In this regard, this paper considered the whole EEP transmission voltage levels. Since voltage instability is a load dependent problem, all 283 load buses are examined, and weakest buses are discussed in detail. Thevenin equivalent parameters seen by load buses are also calculated, which can also be used for other power system analysis studies. The maximum active power transfer capability of the load buses is, also, shown under different system loading scenarios.

2. Method of Analysis

A power system accommodates load increment up to the point of maximum power transfer capability of a load bus. If loading exceeds this limit, the system enters to voltage instability. Hence, locating the point of maximum active power transfer helps to know how much to go loading before the inception of voltage instability.

The location of maximum active power transfer point, in this work, starts by representing the system by a Thevenin equivalent as shown in Figure 1.

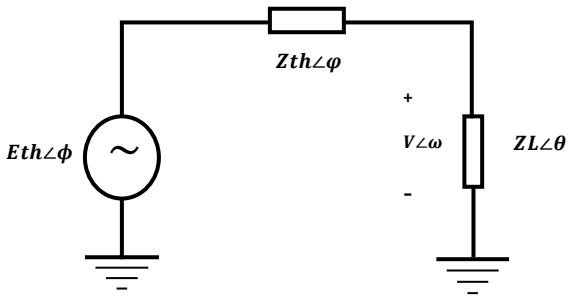

Figure 1. Thevenin equivalent representation of a power system from the load bus.

The Thevenin equivalent system representation is computed by conducting two power flow calculation: one at rated load and the other at full load condition as in [26].

Once, the system Thevenin equivalent is formulated the maximum active power transfer capacity is calculated.

At the maximum power transfer point, we would have the apparent power transferred to the load as:

$$\boldsymbol{S_{@max}} = |I_{@max}|^2 Z_{L@max} \quad (1)$$

According to maximum power transfer theorem, at the point of maximum active power transfer the Thevenin impedance seen by the load matches with the load impedance.

Hence, at this point $Z_{L@max} = |Z_{th}|\angle\theta$ and $I_{@max} = \frac{Eth}{Z_L+Z_{th}} = \frac{Eth}{Z_{th}\angle\theta + Z_{th}\angle\varphi}$. Substituting these values to (1):

$$\boldsymbol{S_{@max}} = \left|\frac{E_{th}\angle\phi}{Z_{th}\angle\theta + Z_{th}\angle\varphi}\right|^2 Z_{th}\angle\theta \quad (2)$$

Computing the squared term:

$$\boldsymbol{S_{@max}} = \frac{E_{th}^2}{Z_{th}((\cos\theta + \cos\varphi)^2 + (\sin\theta + \sin\varphi)^2)}\angle\theta \quad (3)$$

Further simplification will give:

$$\boldsymbol{S_{@max}} = \frac{E_{th}^2}{2Z_{th}(\cos(\varphi - \theta) + 1)}\angle\theta \quad (4)$$

Splitting $\boldsymbol{S_{@max}}$ to active and reactive component we will get the maximum active power transfer as:

$$P_{max} = \frac{E_{th}^2 \cos\theta}{2Z_{th}(\cos(\varphi - \theta) + 1)} \quad (5)$$

$$Q_{@max} = \frac{E_{th}^2 \sin\theta}{2Z_{th}(\cos(\varphi - \theta) + 1)} \quad (6)$$

Eq. (5) tells the maximum active power transfer is dependent on the load side parameter, power factor and the system side parameters, Thevenin parameters. Thevenin parameters represent system configuration.

If the power factor is maintained constant the maximum active power transfer is independent of the amount of the connected load. For pure resistive load, i.e. unity power factor, the maximum power transfer is dependent only on the system configuration.

Once the Thevenin parameters of the system from a load bus is determined, the PV curve of the load bus can be drawn based on the following relation:

$$V = \sqrt{\frac{-v_{term} \pm \sqrt{v_{term}^2 - 4{Z_{th}}^2 S^2}}{2}} \quad (7)$$

Where the voltage term, $v_{term} = 2(PR_{th} + QX_{th}) - E_{th}^2$; The derivation is given in appendix A.

Once the maximum active power transfer is obtained, the stability index is formulated as a normalized difference between current operating active power and the maximum active power transfer as:

$$PPMI = \frac{P_{max} - P_{oper}}{P_{max}} \quad (8)$$

The index (PPMI) measures the distance of current operating point from the critical point in terms of active power, based on the capacity of each load bus. PPMI assumes values from 0 to 1. A value near to zero mean more unstable bus, while value near to 1 mean a more voltage stable load bus.

The procedure followed to assess EEP system voltage stability assessment can be summarized in the following flow chart of Figure 2.

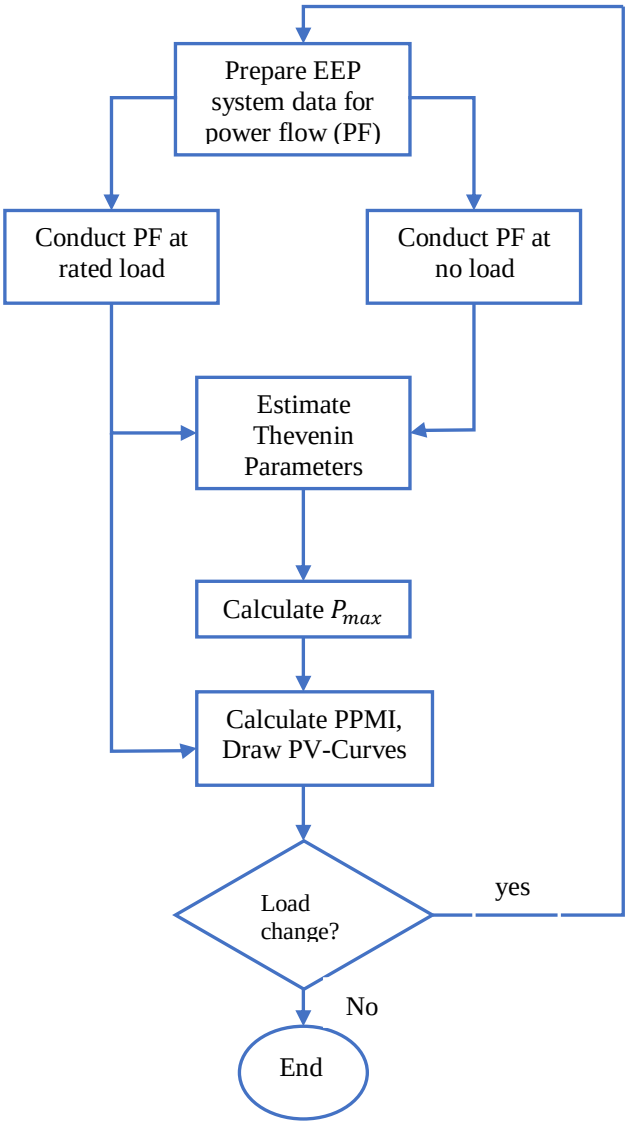

Figure 2. The process followed to assess static voltage stability of EEP system

3. Simulation setup

For the simulation both Matpower 7.1 and Matlab 2021 version software are utilized. Matpower is an open-source power simulation software, used for power flow analysis and run on a Matlab environment. This power system analysis software doesn't employ a graphical representation of a power system. Instead, the power system data is prepared in a table format specific to Matpower [33].
Any functions of the Matpower can, easily, be accessed by functions developed on Matlab editor. In our simulation case, functions regarding to Thevenin equivalent calculation, maximum power calculation and index calculator are developed on Matlab editor and power flow analysis is performed using Matpower.
For this simulation case, the interaction between the software is shown here below in figure 3.

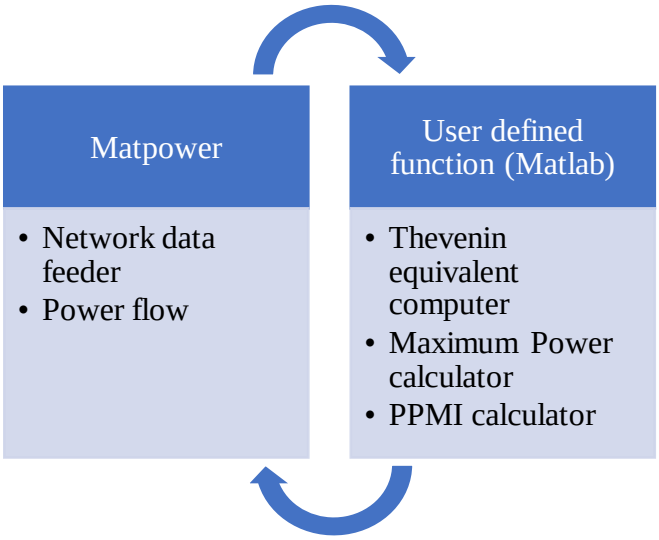

Figure 3. The interaction of the software employed and the developed functions for the simulation

The simulation is performed in the following procedure.

1. EEP data is prepared in Matpower data format. The size of the system taken is given in Table 1 next. Components temporarily or permanently down due to maintenance issue and new components waiting future connectivity are not considered.
   The EEP network is divided into 11 areas. The areas are used by the system operator for both technical and institutional administration. For this work the areas are used latter in the discussions.
2. Power flow is performed using Matpower. To avoid power flow divergence problem progressive scale up of generation and load is employed.
3. Thevenin equivalent representation of the system seen by the load buses is calculated. For this purpose, in addition to the power flow performed above, another power flow is performed with no load at the bus for which the Thevenin equivalent is sought.
4. Next the maximum active power transfer limit of the load buses is calculated.
5. Finally, using the maximum active power transfer limit and the current operating active power the voltage stability index is calculated.

Table 1: Size of the EEP system taken for the simulation

Component	Type	Amount per type	Total amount
Buses	Load buses	283	798
	Generator bus	47	
	Intermediate buses	468	
Transmission lines	500 kV	4	372
	400 kV	30	
	230 kV	130	
	132 kV	160	
	66 kV	34	
	45 kV	13	
	15 kV	1	
Transformers	2 winding	354	575
	3 winding	221	
Generators	Generating units	64	64
Reactive power auxiliary supplies	Shunt capacitors	28	96
	Shunt reactors	68	

Voltage stability investigation is made for four operation scenarios of the EEP system, which are representatives of the EEP system operation of voltage stability concern;

(i) Heavy load uncompensated system
(ii) Heavy load compensated system
(iii) Light load uncompensated system
(iv) Light load compensated system

According to the data accessed from EEP as of 2021, the heavy load operation is taken 75 % of the total connected load, and light load to be 50 % of the total connected load. The total peak load is about 2900 MW including power sales to Sudan and Djibouti. System compensation comes from existing shunt capacitors of capacity 567.2 MVar.

4. Tests and results

The developed index is first tested on IEEE 30 bus system, to validate its functionality. Then it gets deployed on EEP system analysis.
In the analysis, Thevenin equivalent impedance, maximum possible power transfer and the active power margin index are, procedurally, investigated.

4.1. Performance of the index on IEEE 30 bus system

First, the Thevenin parameters are determined. Thevenin equivalent parameters are the important components used for calculating the maximum active power transfer limit. The results are demonstrated using bar graphs in Figure 4.

We can see from the diagram the highest Thevenin impedance is seen by bus 30 followed by bus 26. The minimum Thevenin impedance is seen by bus 4. The Thevenin impedance depends on the admittance matrix and the load current. The whole range of variation in Thevenin impedance, arises from variation in these parameters. The per unit Thevenin voltage doesn't show large pu variations.

Then the maximum active power transfer capacity of each load bus is computed. The highest maximum active power transfer capacity is owned by bus 4, with per unit value of 4.1577 at a critical voltage of 0.6182 pu. The lowest maximum active power transfer capacity is showed by bus 26 with a value of 0.3188 pu at a critical voltage of 0.5330 pu. The lowest critical voltage is also shown by this bus.

The stability index is shown in the bar chart in Figure 5. For comparing the result from the index, other indices ISI and SPMI are shown together in the graph. The result reveals bus 30 to be the weakest bus followed by bus 8. Bus 3 is the strongest bus. Both SPMI and ISI confirm the same result. This result is also proved by other studies made on the same system [27].

Additionally, from the results we can deduce;

- The strongest bus not necessarily have the highest maximum active power transfer capability, vice versa for the weakest bus.
- The weakest bus is not necessarily the one that see the highest Thevenin impedance, and the strongest bus is not necessarily the one which see lowest Thevenin impedance.
- The weakness and strength of the load buses depend on the gap between current operating active power and the maximum active power transfer capability of the bus. The highest the gap, the more voltage stable the bus will be.

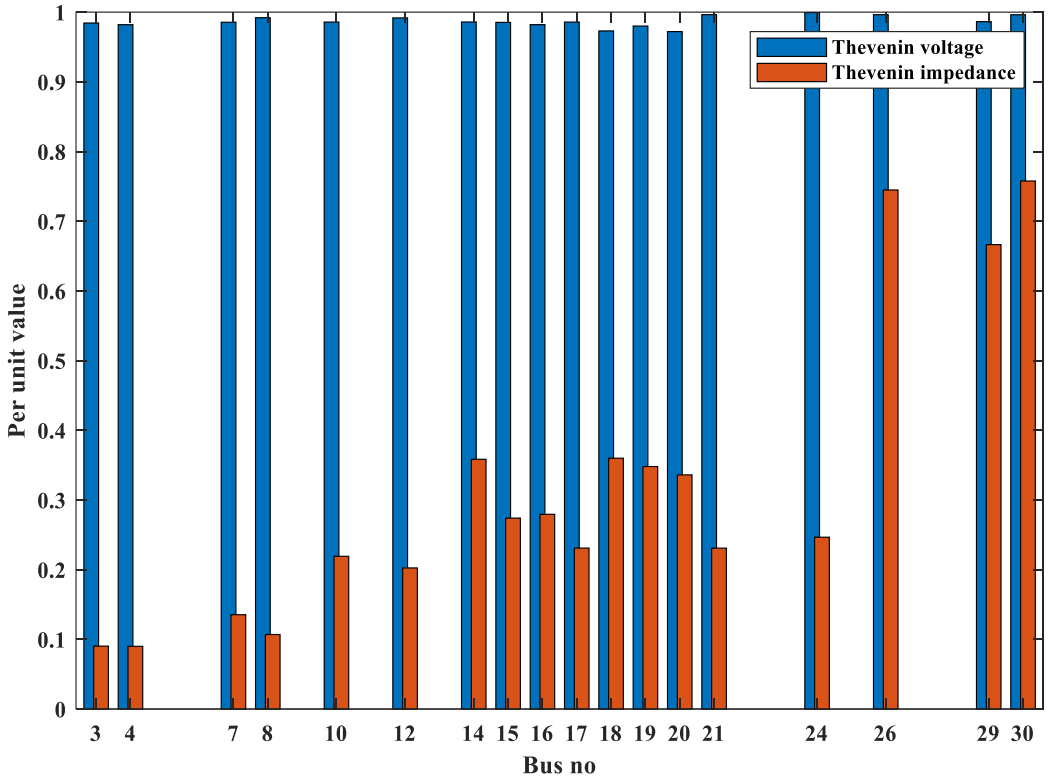

Figure 4. Thevenin equivalent parameters seen by the load buses of IEEE 30 bus system

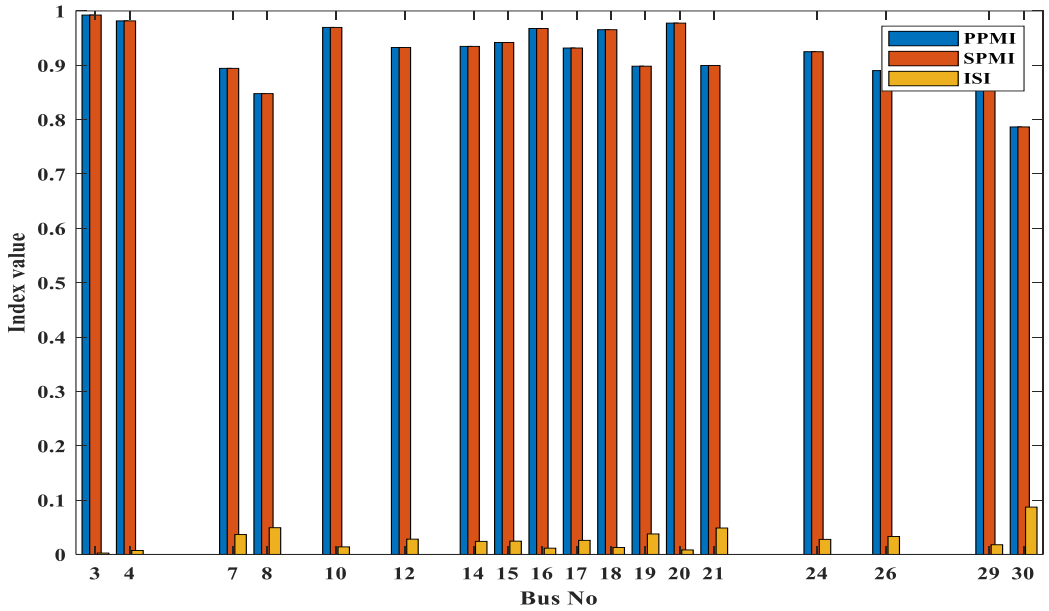

Figure 5. Stability indices for IEEE 30 bus test system

4.2. Investigating the Ethiopian power system

a) Thevenin equivalent impedance

The four scenarios, mentioned before, reveal the dependency of Thevenin impedance on the system unique loading condition. This is shown in bar diagrams of Figure 6 below.

Load increment and reactive power compensation show a differing impact on high value and low value Thevenin impedances.

For a closer investigation of Figure 6, top five and lower five values are screened out in Table 2 below. In the case of high value Thevenin impedance, compensation reduces Thevenin impedance while system load increment increases it. These changes also affect the order of values among the load buses. In the low value Thevenin impedances, for the majority of the buses, compensation increases Thevenin impedance while load increment decreases the Thevenin impedance value.

The largest Thevenin impedances are seen by load buses 225 and 229 consecutively. These two buses are located on the Two terminals of a three-winding transformer. This is an indication of buses near to each other see almost a closer Thevenin impedance values. The buses, seeing high Thevenin impedance values, are those that are supplied from 66 kV transmission line. Area-wise, 70 percent of the top ten Thevenin impedance seeing load buses are from area 7 or area 6.

Table 2. High value and low value Thevenin impedances

	Light load uncompensated system			**Light load compensated system**			**Heavy load uncompensated system**			**Heavy load compensated system**		
High value Thevenin impedance	Load bus	Area	Zth (pu)	Load bus	Area	Zth (pu)	Load bus	Area	Zth (pu)	Load bus	Area	Zth (pu)
	225	7	3.4929	225	7	3.4779	225	7	3.9563	225	7	3.8436
	229	7	3.4808	229	7	3.4672	229	7	3.8902	229	7	3.7923
	176	5	2.3271	176	5	2.3261	204	6	2.4127	204	6	2.3686
	169	5	2.3261	169	5	2.3251	176	5	2.3419	176	5	2.3399
	198	6	2.2829	198	6	2.2800	169	5	2.3412	169	5	2.3392
Low value Thevenin impedances	136	3	0.1004	136	3	0.1008	136	3	0.1004	136	3	0.1004
	121	3	0.1122	121	3	0.1122	121	3	0.1124	121	3	0.1123
	128	3	0.1354	128	3	0.1360	128	3	0.1348	128	3	0.1350
	13	1	0.1615	13	1	0.1654	228	7	0.1517	228	7	0.1554
	17	1	0.1792	227	7	0.1823	13	1	0.1599	13	1	0.1637

On the other hand, buses seeing low Thevenin impedance are buses 136 and 121. The least five values are of buses, which are supplied from either 132 kV or 230 kV transmissions. With some exceptions as in the least three, low Thevenin impedance seeing buses are dominantly from Addis Ababa region, i.e area 1. This can be seen by screening least 20 values. This attributes to the high connectivity of the transmission buses in this area.

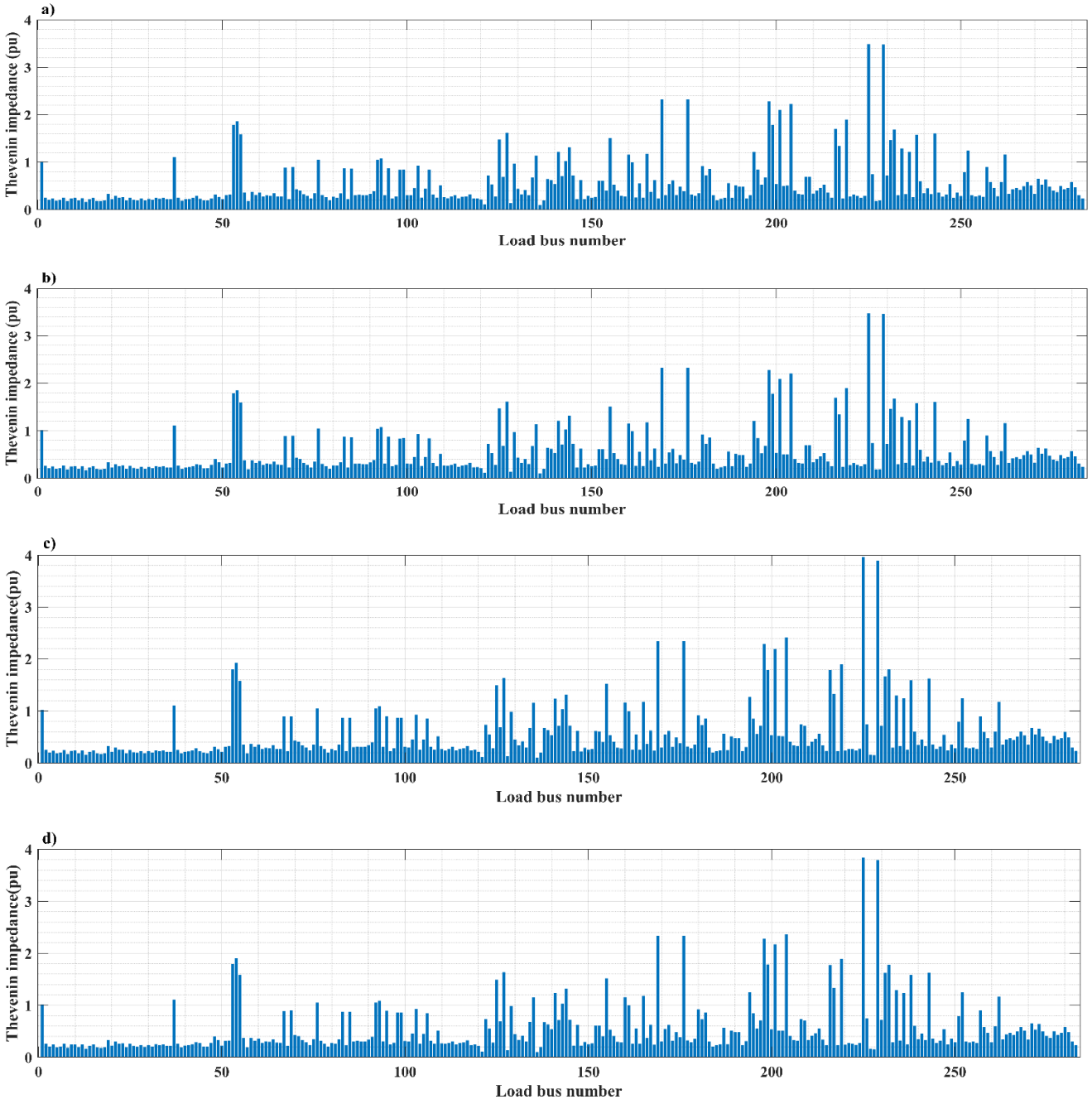

Figure 6. Thevenin impedance seen by the load buses a) Light load uncompensated system b) Light load compensated system c) Heavy load uncompensated system d) Heavy load compensated system

b) Maximum active power transfer (Pmax)

For a given load bus, Pmax changes with load variation of the rest system. Under the four scenarios, the maximum active power transfer capability of the load buses is shown in Figure 7 below.

The results show, as system loading increases the maximum power transfer decreases. This attributes to the reduction of the Thevenin equivalent voltage and the relative increase of Thevenin impedance, with increased system loading. On the other hand, reactive power compensation, i.e. increase in power factor, increases the maximum active power transfer. Compensation, also, can affect the order of Pmax values among load buses.

.

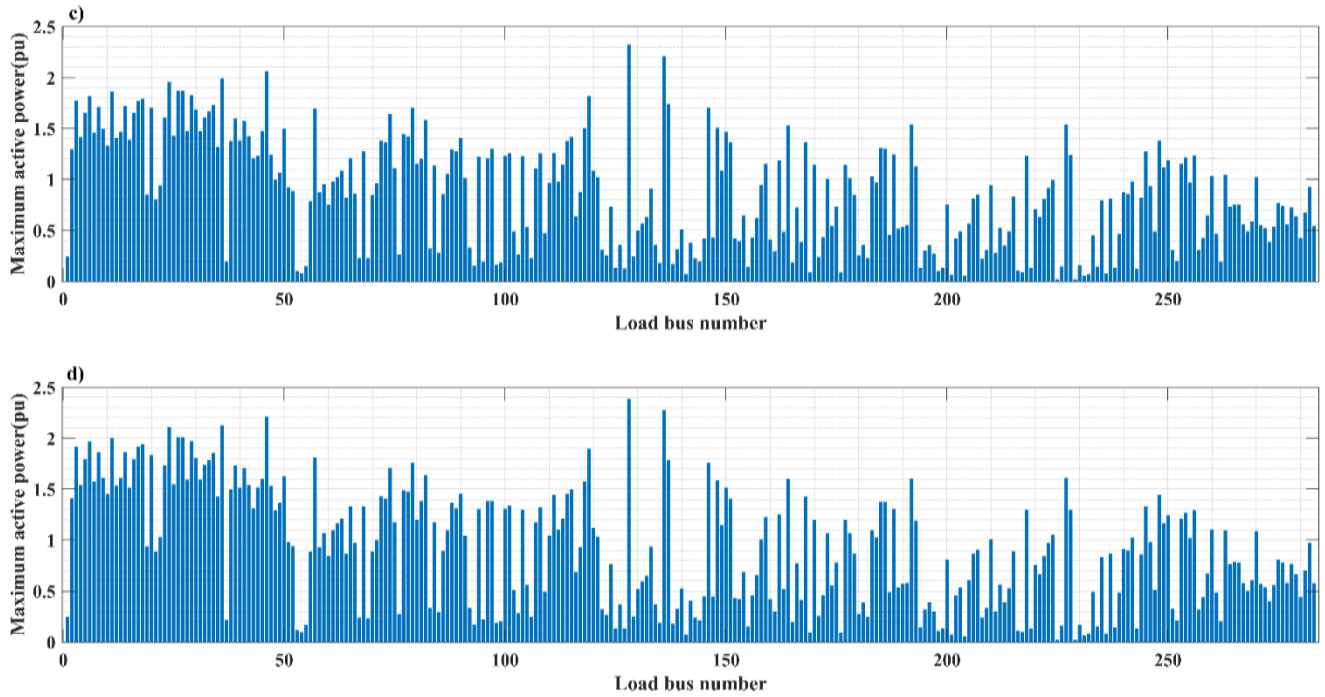

Figure 7. Maximum active power transfer limit of the load buses a) Light load uncompensated system b) Light load compensated system c) Heavy load uncompensated system d) Heavy load compensated system

The investigation also reveals, buses, sharing the same node, show a close Pmax value. This is due to the dependency of the maximum active power transfer on the network representation, as viewed from the load bus independent of the amount of the load connected to the bus.

Top five Pmax values and least five Pmax values are shown below in Table 3. Under all the scenarios load bus 128 owns the highest Pmax value, followed by bus 136. Buses with top Pmax values are supplied from 132 kV and 230 kV transmission lines. On the other hand, bus 225 has the least Pmax value followed by bus 229. Among the least ten Pmax values 80 % of the load buses are supplied from 66 kV transmission lines. More than 80 % of high Pmax value buses are concentrated at area 1, which is at the centre, while the low Pmax values are on the peripheral areas. Buses with lowest Pmax value are frequent in area 7 and area 6. This is due to the high concentration of the 66 kV transmission lines in these areas.

Table 3. Highest and lowest Pmax values under the four scenarios

	Light load uncompensated system			**Light load compensated system**			**Heavy load uncompensated system**			**Heavy load compensated system**		
High Pmax values	Load bus	Area	Pmax (pu)	Load bus	Area	Pmax (pu)	Load bus	Area	Pmax (pu)	Load Bus	Area	Pmax (pu)
	128	3	2.4085	128	3	2.4762	128	3	2.3206	128	3	2.3858
	136	3	2.3006	136	3	2.3677	136	3	2.2094	136	3	2.2739
	46	1	2.1555	46	1	2.3066	46	1	2.0598	46	1	2.2113
	36	1	2.0869	24	1	2.2288	36	1	1.9892	36	1	2.127
	24	1	2.0853	36	1	2.222	24	1	1.9577	24	1	2.1062

Low	225	7	0.0395	225	7	0.0419	225	7	0.0201	225	7	0.0235
Pmax	229	7	0.0401	229	7	0.0425	229	7	0.0211	229	7	0.0244
Values	204	6	0.0749	204	6	0.0805	204	6	0.0528	204	6	0.0591
	141	4	0.0777	141	4	0.0828	231	7	0.0568	231	4	0.0650
	201	6	0.0851	201	6	0.0907	201	6	0.0659	201	6	0.0722

c) Active power margin index (PPMI)

The active power margin index of load buses is determined after calculating the maximum active power transfer. The results are depicted in Figure 8 below.

As system loading increases the PPMI decreases. While, compensation increases the PPMI. Loading changes ranking of strength and weakness of load buses. Ranking depends on each unique system loading condition. Upon system loading change, there are buses who maintained their rank while others change. Here below, the weakest buses are shown in Table 4.

Table 4. Weakest buses under different system loading condition

Light load uncompensated system			**Light load compensated system**			**Heavy load uncompensated system**			**Heavy load compensated system**		
Load bus	area	PPMI	Load bus	area	PPMI	Load bus	area	PPMI	Load bus	area	PPMI
219	7	0.7038	219	7	0.7154	232	7	0.5145	232	7	0.5638
234	7	0.7276	234	7	0.7385	219	7	0.5555	219	7	0.578
201	6	0.7502	201	6	0.7658	201	6	0.5702	201	6	0.6078
232	7	0.7689	232	7	0.7804	234	7	0.5871	234	7	0.6086
198	6	0.777	198	6	0.7834	229	7	0.6333	198	6	0.6805
53	2	0.7825	53	2	0.8044	198	6	0.6676	229	7	0.6833
55	2	0.8092	199	6	0.8224	53	2	0.6771	53	2	0.7131
199	6	0.817	55	2	0.8279	225	7	0.6794	225	7	0.7252
103	2	0.825	103	2	0.8358	231	7	0.6905	231	7	0.7293
263	9	0.841	263	9	0.8471	55	2	0.7202	199	6	0.7378

Based on the 10 weakest buses shown in Table 4 above, the majority of load buses under light load and all the load buses under heavy load condition are supplied from the 66 kV transmission line. The 66kV transmission lines are oldest lines with higher line resistances per km as compared with other transmission lines. This condition of the transmission lines assures the result from PPMI to be reasonable.

From previous discussions, we have seen these buses having large Thevenin impedance and lower Pmax values. These two conditions are also indicators of the possibility for these buses to be weak buses.

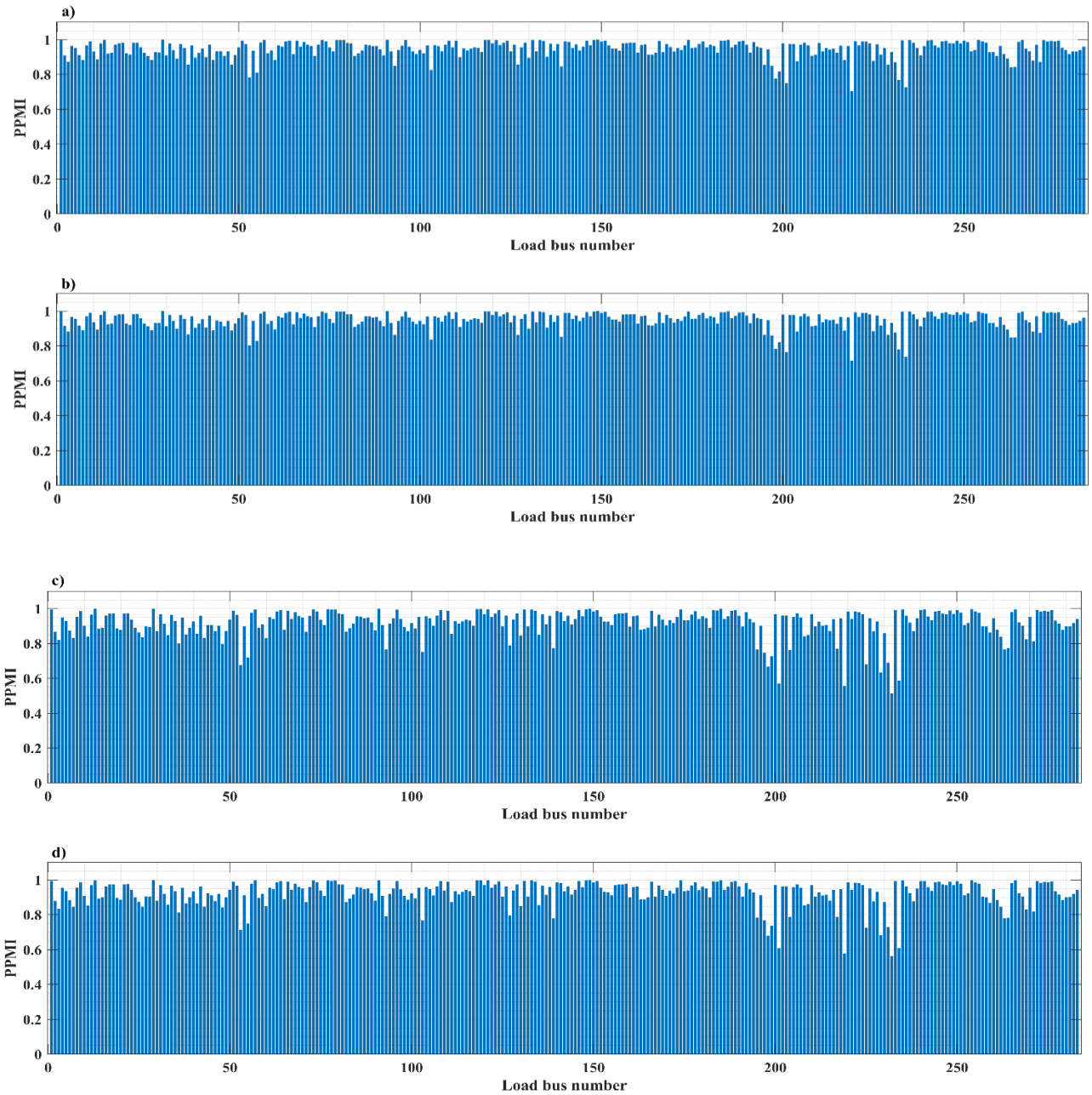

Figure 8. Active power margin index under different loading condition; a) Light load uncompensated system b) Light load compensated system c) Heavy load uncompensated system d) Heavy load compensated system

Speaking area-wise area 7 is the weakest area constituting 60 % of the 10 weakest buses. This area is known not being the most loaded area. Hence, the problem is from the network setup of the area. The high concentration of the 66 kV transmission lines in this area is one of the causes. Hence, considering upgrading these transmission lines is vital for the system voltage stability.

Here below in Figure 9 the PV curves of the four weakest buses are shown.

In the PV diagrams, current operating active power-voltage value is shown by red circles. The four buses have different maximum active power value and current operating values. From the four buses Bus 234 has the highest Pmax value followed by Bus 219, while Bus 201 own the least value. Both Bus 219 and Bus 234 have the highest operating power among the four. The operating power is almost a similar for these two buses. The difference in Pmax created the difference in weakness rank. Bus 219 is the bus with the least operating power among the four.

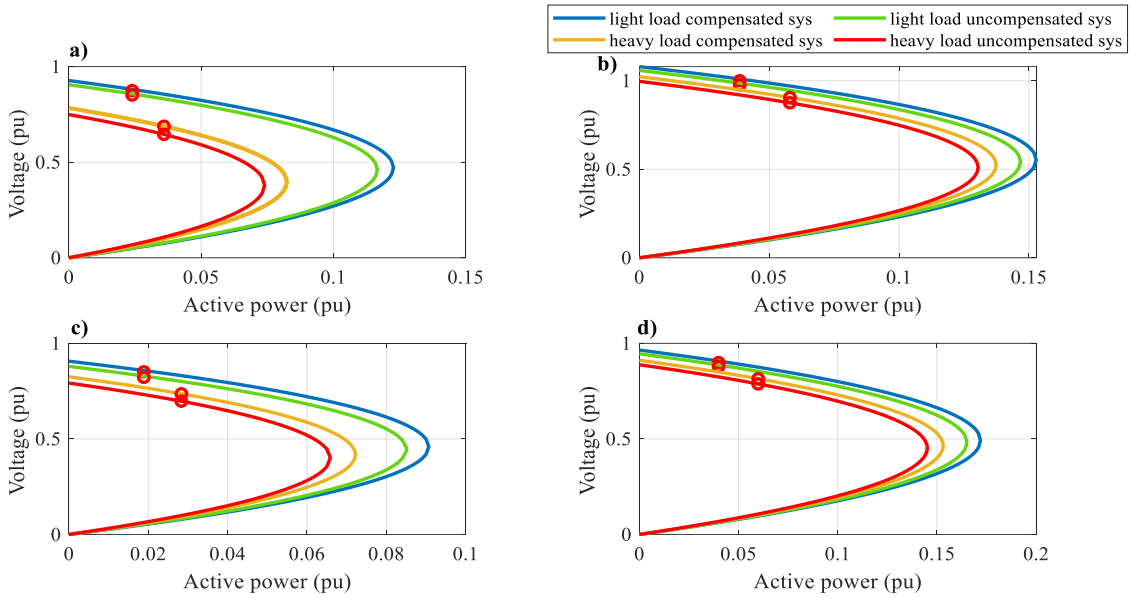

Figure 9. PV diagrams of the weakest buses a) bus 232 b) bus 219 c) bus 201 d) bus 234

The PV diagrams also reveal, system reactive power compensation is improving the voltage profile at current operating active power and seen maximizing the maximum active power transfer. This goes in line with the fact that reactive power compensation improves both low voltage profiles as well as voltage stability.

High system loading reduces both bus voltage profiles and the maximum active power transfer. Decreasing maximum active power transfer against increasing bus loading, results in further reduced active power margin, i.e reduced PPMI.

As it can be seen from Figure 9, for some buses like bus 219 and 234, both loading and reactive power compensation bring comparable impact on the voltage profile and voltage stability level. While for other buses, like 232 and 201, the impact of loading overwhelms the impact of reactive power compensation.

Here it is important to mention PV diagrams cannot be used for bus ranking, for each bus has its unique current operating state and unique maximum active power transfer capability. This is why the index development is necessary.

The most stable buses based on the index are shown here below in Table 5. Top ten buses are selected for demonstration. For the strongest buses the rank change that comes from compensation and loading variation is few. The majority of buses are supplied from 132 kV transmission lines. Buses 149 and 29 are the strongest buses consecutively. The majority of the most stable buses are from area 2 which is located next to the centre of the EEP interconnected system.

The centre, area 1, despite having buses with the highest Pmax and lowest Thevenin impedance, is not the area with the most stable buses. This is due to the fact; area 1 is the most loaded area. This high loading cancels out the advantage of having high Pmax value.

Table 5. The most stable buses under different system loading condition

Light load uncompensated system			**Light load compensated system**			**Heavy load uncompensated system**			**Heavy load compensated system**		
Load bus	Area	PPMI	Load bus	Area	PPMI	Load bus	Area	PPMI	Load bus	Area	PPMI
29	1	0.9995	149	4	0.9996	149	4	0.9994	149	4	0.9994
149	4	0.9995	29	1	0.9995	29	1	0.9993	29	1	0.9993
91	2	0.9992	91	2	0.9992	91	2	0.9988	91	2	0.9989
13	1	0.9989	13	1	0.9990	13	1	0.9984	13	1	0.9985
119	2	0.9987	185	5	0.9987	185	5	0.9982	185	5	0.9983
185	5	0.9986	119	2	0.9986	119	2	0.9980	119	2	0.9981
118	2	0.9984	118	2	0.9985	118	2	0.9977	118	2	0.9979
254	8	0.9983	254	8	0.9983	254	8	0.9976	254	8	0.9977
77	2	0.9982	77	2	0.9983	77	2	0.9975	77	2	0.9976
73	2	0.9981	73	2	0.9982	73	2	0.9974	73	2	0.9974

5. Conclusion

In this paper, the static voltage stability of EEP system, under heavy load and light load condition as well as with and without reactive power compensation is investigated. For the investigation an index called active power margin index, which relays on system Thevenin equivalent representation, is devised. The index is tested for validity using IEEE 30 bus test system and compared with other previously developed indices. Our index produced a matching result with these indices.

From EEP system investigation, highest Thevenin impedance seeing, lowest Pmax value having and most unstable buses are found to be supplied from 66 kV transmission lines. Accordingly, bus 232 load bus is found to be the weakest bus followed by bus 219. Area-wise, area 7 and area 6 are areas that contain considerable number of buses that are nearer to voltage instability. The system operator needs to pay close consideration for these areas. Since the main cause of the problems are the high impedance transmission lines of 66 kV, this work also, recommends upgrading these transmission lines to keep the voltage instability at fair far distance. On the other hand, the most voltage stable buses are supplied from 132 kV transmission and the majority are located in area 2. Buses 149 and 29 are the most stable buses according to the assessment.

Appendix A. Derivation of active power voltage relation

From figure 1, we can set the following relation for the apparent power transferred to the load as:

$$\boldsymbol{S} = \boldsymbol{V}\boldsymbol{I}^{*} \tag{A.1}$$

Then, the current flowing through is:

$$\boldsymbol{I} = \frac{E_{th}\angle\phi - V\angle\omega}{Z_{th}\angle\varphi} \tag{A.2}$$

Substituting equation (A.2) to (A.1):

$$\boldsymbol{S} = V\angle\omega\left(\frac{E_{th}\angle\phi - V\angle\omega}{Z_{th}\angle\varphi}\right)^{*} \tag{A.3}$$

We get the apparent power:

$$\begin{aligned}\boldsymbol{S} &= P + jQ \\ &= \frac{VE_{th}\angle(\omega + \varphi - \phi)}{Z_{th}} - \frac{V^2}{Z_{th}}\angle\varphi\end{aligned} \tag{A.4}$$

Letting $\alpha = \omega + \varphi - \phi$ and separating this term to active and reactive component:

$$P = \frac{VE_{th}}{Z_{th}}\cos\alpha - \frac{V^2}{Z_{th}}\cos\varphi \tag{A.5}$$

$$Q = \frac{VE_{th}}{Z_{th}}\sin\alpha - \frac{V^2}{Z_{th}}\sin\varphi \tag{A.6}$$

From the identity:

$$\sin^2\alpha + \cos^2\alpha = 1 \tag{A.7}$$

From equations (A.5), (A.6) and (A.7):

$$\left(\frac{PZ_{th}}{VE_{th}} + \frac{V}{E_{th}}\cos\varphi\right)^2 + \left(\frac{QZ_{th}}{VE_{th}} + \frac{V}{E_{th}}\sin\varphi\right)^2 = 1 \tag{A.8}$$

Rearranging the terms, we come across an equation of quadratic form in V^2 as:

$$V^4 + V^2(2Z_{th}(P\cos\varphi + Q\sin\varphi) - E_{th}^2) + {Z_{th}}^2(P^2 + Q^2) = 0 \quad \text{(A.9)}$$

Then, expressing the reactive power in terms of active power using the power factor angle:

$$Q = P\tan\theta \quad \text{(A.10)}$$

Substituting this equation to equation (A.9):

$$V^4 + V^2(2Z_{th}P(\cos\varphi + \tan\theta\sin\varphi) - E_{th}^2) + {Z_{th}}^2P^2\sec^2\theta = 0 \quad \text{(A.11)}$$

This equation gives four solutions for the voltage among which only two are feasible.

Then solving for V^2 and using Thevenin impedance terms:

$$V^2 = \frac{-\left(2(PR_{th} + QX_{th}) - E_{th}^2\right)}{2} \pm \frac{\sqrt{\left(2(PR_{th} + QX_{th}) - E_{th}^2\right)^2 - 4{Z_{th}}^2P^2\sec^2\theta}}{2} \quad \text{(A.12)}$$

References

[1] P. Kundur *et al.*, "Definition and classification of power system stability IEEE/CIGRE joint task force on stability terms and definitions," *IEEE Trans. Power Syst.*, vol. 19, no. 3, pp. 1387-1401, 2004, doi: 10.1109/TPWRS.2004.825981.

[2] N. Hatziargyriou *et al.*, "Definition and Classification of Power System Stability – Revisited & Extended," *IEEE Trans. Power Syst.*, vol. 36, no. 4, pp. 3271-3281, 2021, doi: 10.1109/TPWRS.2020.3041774.

[3] J. W. Simpson-Porco, F. Dörfler, and F. Bullo, "Voltage collapse in complex power grids," *Nat. Commun.*, vol. 7, no. 1, p. 10790, 2016/02/18 2016, doi: 10.1038/ncomms10790.

[4] M. Glavic *et al.*, "See It Fast to Keep Calm: Real-Time Voltage Control Under Stressed Conditions," *IEEE Power Energy Mag.*, vol. 10, no. 4, pp. 43-55, 2012, doi: 10.1109/MPE.2012.2196332.

[5] T. Van Cutsem and C. Vournas, *Voltage stability of electric power systems*. Springer Science & Business Media, 2007.

[6] Y. Ma, S. Lv, X. Zhou, and Z. Gao, "Review analysis of voltage stability in power system," in *2017 IEEE International Conference on Mechatronics and Automation (ICMA)*, 6-9 Aug. 2017 2017, pp. 7-12, doi: 10.1109/ICMA.2017.8015779.

[7] M. S. S. Danish, T. Senjyu, S. M. S. Danish, N. R. Sabory, N. K, and P. Mandal, "A Recap of Voltage Stability Indices in the Past Three Decades," *Energies*, vol. 12, no. 8, p. 1544, 2019. [Online]. Available: https://www.mdpi.com/1996-1073/12/8/1544.

[8] S. L. Y. Ma, X. Zhou and Z. Gao, , "Review analysis of voltage stability in power system," in *International Conference on Mechatronics and Automation*, 2017.

[9] M. Begovic, B. Milosevic, and D. Novosel, "A novel method for voltage instability protection," in *Proceedings of the 35th Annual Hawaii International Conference on System Sciences*, 10-10 Jan. 2002 2002, pp. 802-811, doi: 10.1109/HICSS.2002.993968.

[10] B. Gao, G. K. Morison, and P. Kundur, "Voltage stability evaluation using modal analysis," *IEEE Trans. Power Syst.*, vol. 7, no. 4, pp. 1529-1542, 1992, doi: 10.1109/59.207377.

[11] H. J. Chen, T.; Yuan, H.; Jia, H.; Bai, L.; Li, F. , "Wide-area measurement-based voltage stability sensitivity and its application in voltage control," *Int. J. Electr. Power Energy Syst.*, vol. 88, pp. 87-98, 2017.

[12] T. P. C. Hai, H.; Chung, I.Y.; Kang, H.K.; Cho, J.; Kim, J, "A novel voltage control scheme for low-voltage DC distribution systems using multi-agent systems," *Energies*, vol. 10, pp. 14-19, 2017.

[13] H.Glavitsch, "Estimating the Voltage Stability of a Power System," *IEEE Trans. Power Deliv.*, vol. PWRD-1, N3, July 1986, doi: 10.1109/TPWRD.1986.4308013.

[14] I. Musirin and T. K. A. Rahman, "Novel fast voltage stability index (FVSI) for voltage stability analysis in power transmission system," in *Student Conference on Research and Development*, 17-17 July 2002 2002, pp. 265-268, doi: 10.1109/SCORED.2002.1033108.

[15] U. K. Sultana, A.B.; Aman, M.M.; Mokhtar, A.S.; Zareen, N. , "A review of optimum DG placement based on minimization of power losses and voltage stability enhancement of distribution system," *Renewable and Sustainable Energy Reviews* vol. 63, pp. 363–378, September, 2016.

[16] H. S. Salama and I. Vokony, "Voltage stability indices–A comparison and a review," *Comput. Electr. Eng.*, vol. 98, p. 107743, 2022/03/01/ 2022, doi: https://doi.org/10.1016/j.compeleceng.2022.107743.

[17] E. G. C. P. R.B. Prada, J.O.R. dos Santos , A. Bianco, L.A.S. Pilotto "Voltage stability assessment for real-time operation," *IEE Proceedings - Generation, Transmission and Distribution*, vol. Volume 149, no. Issue 2, pp. 175 – 181, March 2002, doi: 10.1049/ip-gtd:20020282.

[18] M. Kamel, F. Li, S. Bu, and Q. Wu, "A generalized voltage stability indicator based on the tangential angles of PV and load curves considering voltage dependent load models," *Int. J. Electr. Power Energy Syst.*, vol. 127, p. 106624, 2021/05/01/ 2021, doi: https://doi.org/10.1016/j.ijepes.2020.106624.

[19] S. G. Ghiocel and J. H. Chow, "A Power Flow Method Using a New Bus Type for Computing Steady-State Voltage Stability Margins," *IEEE Trans. Power Syst.*, vol. 29, no. 2, pp. 958-965, 2014, doi: 10.1109/TPWRS.2013.2288157.

[20] V. Ajjarapu and C. Christy, "The continuation power flow: a tool for steady state voltage stability analysis," *IEEE Trans. Power Syst.*, vol. 7, no. 1, pp. 416-423, 1992, doi: 10.1109/59.141737.

[21] A. B. N. Elisabete de Mello Magalhães, Dilson Amancio Alves,, "A Parameterization Technique for the Continuation Power Flow Developed from the Analysis of Power Flow Curves," *Math. Probl. Eng.*, vol. 2012, p. 24 pages, 2012, Art no. 762371, doi: https://doi.org/10.1155/2012/762371.

[22] K. Karthikeyan and P. K. Dhal, "Multi verse optimization (MVO) technique based voltage stability analysis through continuation power flow in IEEE 57 bus," *Energy Procedia*, vol. 117, pp. 583-591, 2017/06/01/ 2017, doi: https://doi.org/10.1016/j.egypro.2017.05.153.

[23] R. Pourbagher, S. Y. Derakhshandeh, and M. E. Hamedani Golshan, "An adaptive multi-step Levenberg-Marquardt continuation power flow method for voltage stability assessment in the Ill-conditioned power systems," *Int. J. Electr. Power Energy Syst.*, vol. 134, p. 107425, 2022/01/01/ 2022, doi: https://doi.org/10.1016/j.ijepes.2021.107425.

[24] C. Liu, A. Bose, M. Han, and X. Chen, "Improved continuation power flow method for AC/DC power system," in *2011 IEEE Electrical Power and Energy Conference*, 3-5 Oct. 2011 2011, pp. 192-198, doi: 10.1109/EPEC.2011.6070194.

[25] D. K. Molzahn, B. C. Lesieutre, and H. Chen, "Counterexample to a Continuation-Based Algorithm for Finding All Power Flow Solutions," *IEEE Trans. Power Syst.*, vol. 28, no. 1, pp. 564-565, 2013, doi: 10.1109/TPWRS.2012.2202205.

[26] A. Hilawie and F. Shewarega, "Developing New Thevenin Impedance Determination Technique and Voltage Stability Assessment Index for Online Application," in *2021 IEEE PES/IAS PowerAfrica*, 23-27 Aug. 2021 2021, pp. 1-5, doi: 10.1109/PowerAfrica52236.2021.9543381.

[27] Y. Wang *et al.*, "Voltage Stability Monitoring Based on the Concept of Coupled Single-Port Circuit," *IEEE Trans. Power Syst.*, vol. 26, no. 4, pp. 2154-2163, 2011, doi: 10.1109/TPWRS.2011.2154366.

[28] U. P. Africa. "Ethiopia's energy sector review: Fact Sheet." www.usaid.gov/ powerafrica/Ethiopia (accessed April, 5, 2022).

[29] W. bank. "World bank data." https://data.worldbank.org/indicator/EG.ELC.LOSS.ZS?locations=ET (accessed April 10, 2022).

[30] T. Van Cutsem, "Voltage instability: phenomena, countermeasures, and analysis methods," *Proc. IEEE*, vol. 88, no. 2, pp. 208-227, 2000.

[31] M. A. G. Biru, "Analysis of the Power Blackout in the Ethiopian Electric Power Grid," *Sci. j. circuits syst. signal process*, vol. 8, no. 2, pp. 53-65, December 2019, doi: 10.11648/j.cssp.20190802.14.

[32] T. G. Tella, S. S. Sitati, and G. N. Nvakoe, "Voltage Stability Assessment on Ethiopian 230 KV Transmission Network Using Modified Voltage Stability Indices," in *2018 IEEE PES/IAS PowerAfrica*, 28-29 June 2018 2018, pp. 1-5, doi: 10.1109/PowerAfrica.2018.8521144.

[33] R. D. Zimmerman, C. E. Murillo-Sánchez, and R. J. Thomas, "MATPOWER: Steady-State Operations, Planning, and Analysis Tools for Power Systems Research and Education," *IEEE Trans. Power Syst.*, vol. 26, no. 1, pp. 12-19, 2011, doi: 10.1109/TPWRS.2010.2051168.